Factors that discriminate invasive adenocarcinoma from minimally invasive adenocarcinoma and adenocarcinoma in situ in patients with pure ground-glass pulmonary nodules

Huan-Huan Yang
Shanghai Jiao Tong University Affiliated Chest Hospital
Yi-Lv Lv
Shanghai Jiao Tong University Affiliated Chest Hospital
Xing-Hai Fan
shanghai zhongye hospital
Zhi-Yong Ai
shanghai zhongye hospital
Xiu-Chun Xu
shanghai zhongye hospital
Bo Ye (yb1373@shchest.org)
Shanghai Jiao Tong University Affiliated Chest Hospital
Ding-zhong Hu
shanghai chest hospital

Research

Keywords: Adenocarcinoma, ground-glass nodule, prognosis, computed tomography

Posted Date: May 17th, 2020

DOI: https://doi.org/10.21203/rs.3.rs-26727/v1

Version of Record: A version of this preprint was published on July 31st, 2020. See the published version at https://doi.org/10.1186/s13014-020-01628-x.

Abstract

Purpose

The aim of the present study was to investigate predictors of pathological invasiveness and prognosis of lung adenocarcinoma in patients with pure ground-glass nodules (pGGNs).

Methods

Clinical and computed tomography (CT) features of invasive adenocarcinomas (IACs) and pre-IACs were retrospectively compared in 641 consecutive patients with pGGNs and confirmed lung adenocarcinomas who had been followed up by CT postoperatively, and potential predictors of prognosis were investigated.

Results

Of 659 pGGNs in 641 patients, 258 (39.1%) were adenocarcinomas *in situ*, 265 (40.2%) were minimally invasive adenocarcinomas, and 136 (20.6%) were IACs. Respective optimal cutoffs for age, serum carcinoembryonic antigen, maximal diameter, mean diameter, and CT density for distinguishing preIACs from IACs were 53 years, 2.19 ng/mL, 10.78 mm, 10.09 mm, and − 582.28 Hounsfield units (HU). In univariable analysis sex, age, maximal diameter, mean diameter, CT density, and spiculation were significant predictors of lung IAC. In multivariable analysis age, maximal diameter, and CT density were significant predictors of lung IAC. During a median follow-up of 41 months no pGGN IACs recurred.

Conclusions

pGGNs may be lung IACs, especially in patients aged > 55 years with lesions that are > 1 cm in diameter and exhibit CT density > − 600 HU. pGGN IACs of < 3 cm in diameter have good post-resection prognoses. These data may assist the selection of surgical procedures in patients with pGGNs at high risk of malignancy.

Introduction

In computed tomography (CT) images pure ground-glass nodules (pGGNs) are visualized as homogeneous hazy lesions of the lung in which the vascular and bronchial components are preserved and there is no solid component. The use of CT to screen for lung cancer has resulted in detection of an increasing number of pGGNs[1], which are consistently found to constitute precursors of lung invasive adenocarcinomas (IACs). pGGNs include atypical adenomatous hyperplasia, adenocarcinoma *in situ* (AIS), and minimally invasive adenocarcinoma (MIA) [2–4]. These lesions often grow slowly and have good prognoses[5–8]. Many pGGNs > 1 cm in diameter eventually develop into IACs however, which have a poorer prognosis [9]and thus require different therapeutic strategies [10–11]. Therefore, the ability to

detect these IACs preoperatively on the basis of clinical manifestations and CT characteristics is beneficial. The purpose of the current study was to identify factors that discriminated IACs from MIAs and AISs in patients with pGGNs who had undergone surgical resection, and determine their prognoses.

Materials And Methods

Study design

The study was conducted in accordance with the Declaration of Helsinki. The Institutional Review Board and the Ethics Committee of Shanghai Chest Hospital approved the study, and waived the requirement for patient consent due to its retrospective design.

Patients

A search of the electronic medical records of Shanghai Chest Hospital yielded 5,748 consecutive patients with a pathological diagnosis of lung cancer who had undergone surgical resection at the Department of Thoracic Surgery between January 2014 and December 2015. Inclusion criteria were (1) availability of pre-resection CT; (2) lesions manifesting as pGGNs on CT; (3) lesions < 3 cm in diameter as determined via CT; and (4) pathologically verified lung adenocarcinoma. The final sample included 641 patients with 659 pGGNs.

Preoperative data

The data collated included age, sex, smoking history (never or current/former), symptoms (none, or any of cough, shortness of breath, fever, hemoptysis, chest pain, recurrent pulmonary infection), serum carcinoembryonic antigen (CEA) concentration, and CT features of all patients. All patients underwent thoracic unenhanced CT examination at our hospital preoperatively. Lung CT scans were performed with a Somatom Sensation-64 (Siemens Medical Systems, Forchheim, Germany) with 120 kVp and 100 mAs. All CT examinations included the entire thorax at full suspended inspiration with the patient lying supine. We routinely performed thin-section scanning CT with 2-mm collimation for all lung nodules < 3 cm in diameter. The lung window width was consistently 1600 Hounsfield units (HU), and the window level was − 600 HU.

Tumor size was expressed as maximal (longest diameter in mm on axial images) and mean (average of long-axis and short-axis diameters obtained on the same image) diameters [12]. CT density was defined as the average CT attenuation (HU) in 10-mm^2 regions of interest at two different sites within the nodule that did not contain blood vessels or bronchioles. For smaller nodules a region of interest that was as large as possible was used to measure density. Two observers (radiologist J.G. with 16 years of experience in chest CT and surgeon J.F. with 12 years of experience in thoracic surgery) who were blinded to the histopathological results and clinical data evaluated all CT scans independently. They each measured the size and density of the lesions in the lung window setting on the transverse CT section that displayed the largest nodule dimensions. The average of the measurements obtained by each of the two reviewers was used for analysis. The observers also recorded the presence of particular signs such as

pleural retraction, air bronchogram, bubble lucency, and spiculated margins. Pleural retraction was defined as linear attenuation heading toward the pleura or the major or minor fissure from a pGGN. Air bronchogram was defined as air-filled bronchi within a pGGN. Bubble lucency was defined as the presence of small spots of round or ovoid air attenuation within a pGGN. Spiculated margins were defined as the presence of strands extending from a nodule margin into the lung parenchyma without reaching the pleural surface[4]. In cases where only one of the two primary observers concluded that the imaging depicted a pGGN, another radiologist (Z.X.G. with 24 years of experience) was consulted and their decision was deemed final.

Histopathological findings

To ensure that the resected nodules corresponded to the nodules seen in the CT scans the radiologic and surgical procedures were conducted on the same day, and CT-guided microcoils were inserted to mark both the nodule and the visceral pleural surface. Intra-operative fluoroscopy was then used to identify the microcoils, and thus the nodule to be resected. Two chest pathologists (F.X.J. with 12 years of experience and Z.H. with 23 years of experience) who were blinded to all clinical information reviewed the pathological specimens independently and classified the lesions as atypical adenomatous hyperplasia, AIS, MIA, or IAC in accordance with the criteria described in the 2015 World Health Organization Classification of Lung Tumors [13–14], and they were able to reach a consensus on all occasions via discussion. They also classified the histological subtypes of IACs as lepidic predominant, acinar predominant, papillary predominant, micropapillary predominant, solid predominant, or invasive mucinous adenocarcinoma and then classified all tumors into two categories; pre-IAC (including AIS and MIA) and IAC.

Statistical analysis

Optimal cutoff values were determined via the maximal Youden index (sensitivity + specificity − 1) using logistic regression. Receiver operating characteristic (ROC) curves were then constructed for age, CEA, maximal and mean diameters, and CT values using the calculated optimal cutoff values and area under the receiver operating characteristic curves (AUCs) to construct ROC curves with adequate sensitivity and specificity. Because we consider integer values more convenient for clinical use, we stratified both maximal and mean diameters as ≤ 10 mm and > 10 mm (the cutoff for maximal diameter was 10.78 mm and the cutoff for mean diameter was 10.09 mm) and CTdetermined density as ≤ − 600 HU and > − 600 HU. With a calculated cutoff value of 53 years for age, we stratified age as ≤ 55 years and > 55 years based on the nearest 5-year interval. Although our cutoff value for CEA was 2.19 μg/L, we used the upper limit of the normal range of 5 μg/L as our standard for stratification.

Relationships between IAC and each variable were compared using the χ^2 test. Because some patients had multiple nodules, the correlated data were accounted for using generalized estimating equations with a logit link function and a binomial distribution to assess relationships between clinicopathological factors and lung IAC. The appropriate working correlation structure was selected according to the quasi-likelihood under the independence model criterion minimum principle, and odds ratios (ORs) and 95%

confidence intervals (CIs) were calculated. Multivariable model 1 was established by including variables with $p < 0.1$ in univariable analysis. All variables were incorporated into model 2. Models 1 and 2 were then compared to assess the stability of the results. Lastly, a multicollinearity test was performed on all independent variables. All statistical analyses were performed with SPSS software version 17.0, and $p < 0.05$ was deemed to indicate statistical significance.

Results

Optimal cutoff values for continuous predictors

The optimal cutoff values and AUCs for age, CEA, maximal and mean diameters, and CTdetermined density for discriminating between pre-IAC and IAC are summarized in Table 1. All data used to derive the sensitivity and specificity values and the positive and negative predictive values shown in Table 1 are provided as electronic supplementary material (ESM Table 1). ROC curve analyses are presented in Fig. 1.

Patient characteristics and radiological and pathological features

There were 659 pGGNs detected in 641 patients, of whom 449 were women and 192 were men. The median age was 62.7 years (range 26–78 years). Eight men and 10 women had two pGGNs. Of the 659 pGGNs 523 (79.4%) were pre-IACs, including 258 (39.2%) AISs and 265 (40.2%) MIAs. The remaining 136 (20.6%) were IACs, including 58 (8.8%) lepidic predominant, 33 (5.0%) acinar predominant, 43 (6.5%) papillary predominant, and 2 (0.3%) solid predominant adenocarcinomas. Figure 2 is a flow chart depicting the process of classifying the nodules. There were no significant differences in CEA concentration ($p = 0.792$), or the frequencies of pleural retraction ($p = 0.857$), air bronchogram signs ($p = 1.000$), or bubble lucency signs ($p = 0.598$) between the pre-IAC group and the IAC group. There were significant differences in the sex distribution ($p = 0.025$), age ($p < 0.001$), CT density ($p < 0.001$), spiculation signs ($p = 0.021$), and mean and maximal diameters (both $p < 0.001$) between these two groups. The relevant data are summarized in Table 2.

Factors predicting IAC

The results of the univariable and multivariable analyses are summarized in Table 3. In univariable analysis IAC was significantly associated with age ($p < 0.001$), sex ($p = 0.024$), mean and maximal diameters (both $p < 0.001$), CT density ($p < 0.001$), and spiculation signs ($p = 0.02$). Maximal nodule diameters are plotted by pathological type in Fig. 3. Of the 523 pre-IACs, 122 (23.3%) were > 10 mm in diameter as determined via CT. Of the 136 IACs, 107 (78.7%) were > 10 mm in diameter as determined via CT. With regard to CT density, 226 (43.2%) of the 523 pre-IACs exhibited CT densities > − 600 HU, and 89 (65.4%) of the 136 IACs exhibited CT densities > − 600 HU. Of the 229 pGGNs that were > 10 mm in diameter as determined via CT, 122 (53.3%) were pre-IACs (41 AISs and 81 MIAs) and 107 (46.7%) were IACs (Kruskal-Wallis test $\chi^2 = 176.488$, $p < 0.001$). pGGN CT densities are plotted by pathological type in

Fig. 4. Of the 315 nodules with a CT density > − 600 HU, 226 (71.7%) were pre-IACs (87 AISs and 139 MIAs) and 89 (28.3%) were IACs (Kruskal-Wallis test $\chi^2 = 45.60$, $p < 0.001$).

In multivariable analysis model 1 which included input variables that had $p < 0.1$ in univariable analysis (sex, age, maximal and mean diameters, CT density, and spiculation signs), age (OR 2.2, 95% CI 1.4–3.7, $p < 0.001$), mean diameter (OR 6.2, 95% CI 2.4–16.4, $p = 0.002$), and CT density (OR 3.5, 95% CI 2.2–5.8, $p < 0.001$) were significant independent factors for differentiating pre-IACs and IACs (Table 3). In multivariable analysis model 2 which included all potential variables and was conducted to assess sensitivity, age (OR 2.7, 95% CI 1.6–4.7, $p < 0.001$), maximal diameter (OR 3.0, 95% CI, 1.1–8.2, $p = 0.032$), mean diameter (OR 4.7, 95% CI 1.8–12.6, $p = 0.002$), and CT density (OR 3.9, 95% CI 2.3–6.5, $p < 0.001$) were significant independent differentiating factors for IAC (Table 3). A multicollinearity test indicated that there were no multicollinearity problems in the multivariable models (Table 4).

All univariable and multivariable analysis results are presented as a forest plot in Fig. 5. Age, maximal diameter, mean diameter, and CT density were all independent factors that distinguished IAC from pre-IAC.

Recurrence of pGGNs

After a median follow-up period of 41 months (range 7–52 months) after resection, no pGGN IACs or pre-IACs had recurred. After the operation, chest CT was periodically conducted and no new nodules were detected.

Discussion

Several studies have analyzed relationships between CT features of pGGNs and pathological type [15–18]. To the best of our knowledge however, no published study has identified predictors of lung IACs in pGGNs by analyzing their clinical and imaging characteristics. In the present study 659 adenocarcinomas manifesting as pGGNs on CT were investigated, making the study larger than most recent studies investigating pathological classification of pGGNs [11, 15, 17, 19–20].

Kitami et al. [15] reported cutoffs of − 600 HU for CT density and 10 mm for maximum diameter for distinguishing between IAC and non-IAC pGGNs of the lung. The corresponding cutoffs identified in the current study are similar to those values, and other previously reported values [11, 15]. Because integers are more convenient, we used published cutoff values in our univariable and multivariable analyses (age > 55 years, maximal diameter > 1 cm, CT density > − 600 HU). In the present study, model 2 suggested that maximal and mean diameters could reliably and independently discriminate IACs in patients with pGGNs with diameters of < 3 cm. Lim et al. [11] reported that pGGN size was a significant indicator when differentiating IACs from AISs and MIAs when the nodules had diameters > 10 mm. Kitami et al. [15] identified a maximal diameter cutoff of 10 mm for distinguishing between lung IACs and non-IACs presenting as pGGNs. Although in the current study a tumor diameter of > 10 mm was a significant

independent predictor of IAC, that result is not readily apparent from the scatter plot shown in Fig. 3. Perhaps the best predictor of IAC may be a diameter of > 20 mm, because only one of the pre-IACs shown in Fig. 3 had a diameter > 20 mm. However, although that threshold would yield a high positive predictive value the corresponding negative predictive value would be abysmal. This would result in a high rate of missed diagnoses in clinical practice. Notably, the observation in the present study that a tumor diameter of > 10 mm was an independent predictor of IAC is consistent with results reported in similar previous studies [17–18, 21–23]. As depicted in the scatter plot of pGGN diameters determined via CT by pathological type shown in Fig. 3, in the current study the more aggressive the histological subtype was the larger the pGGN's diameter tended to be. Thus, tumor size is the most important variable on which to base decisions pertaining to the management of pGGNs [12, 24–25].

Although nodules > 10 mm in diameter are more likely to be IACs, smaller nodules may also be IACs. In the present study 29 nodules with diameters of < 10 mm were found to be IACs. Thus, nodules with diameters of < 10 mm must also be managed and followed up diligently to ensure that malignant changes do not go undetected. We suggest that it is appropriate to monitor nodules with diameters < 10 mm independently. With regard to these smaller nodules, further research is needed to establish a basis for clinical planning.

Although CT-determined density of pGGNs of > − 600 HU was a significant predictor of IAC in the present study, the scatter plot shown in Fig. 4 does not clearly depict this result. We think that using a single factor to predict IACs is not good clinical practice, and the assessment of multiple factors simultaneously would be more accurate. Notably, Kitami et al. [11] reported that the CTdetermined density of pGGNs can distinguish IACs, and Lim et al. [11] reported that pGGN density was a significant predictor of tumor invasiveness. In contrast, Heidinger et al. [17] reported that pGGN density was not significantly associated with pathological diagnosis, and several other groups have also reported no significant differences in nodule density between AISs, MIAs, and IACs manifesting as pGGNs on CT [20–21]. Thus, whether CT density is a valid parameter for distinguishing IACs remains controversial. CT density should be combined with other indicators such as size, patient age, and certain CT signs when predicting the nature of a lesion preoperatively.

Liu et al. [22] reported that the presence of signs of spiculation is suggestive of a diagnosis of IAC. In univariable analysis in the present study spiculation was a significant predictor of IAC; however, this was not confirmed in multivariable analysis. Spiculation is considered to be evidence of malignancy and to represent invasiveness. In one study spiculation was the strongest predictor of invasion [26].

In the present study age was a significant predictor of IAC. To the best of our knowledge no previous studies have identified this correlation. This hitherto unreported result of the current study warrants further investigation in prospective studies. In clinical practice, whether surgical resection is recommended in patients with pGGN who are aged > 55 years is determined with reference to a combination of other additional factors such as nodule diameter and nodule density. IACS presenting as pGGNs have a good prognosis. In the present study, no pGGN IACs recurred after surgical resection during

a median follow-up period of 41 months (range 7–52 months), a finding that is consistent with some previous research [27–29] .

It is well established that IACs and pre-IACs require treatment via different surgical procedures. At our hospital surgery is performed if the diameter of the pGGN is > 8 mm. Most patients are treated via limited resection and frozen section, and lobectomy is performed if an invasive component is detected via frozen section. Unfortunately, the accuracy of frozen section is not satisfactory [30]. Moreover, the distinction between MIA and IAC is still difficult even if invasive components are observed. Because the accuracy of intraoperative frozen sections is still unclear, it is easier to determine the appropriate treatment if IAC can be predicted accurately. Although limited resection is the preferred treatment for pGGN, it may not be possible to remove all lesions. In the present study 20.6% of pGGNs were eventually diagnosed as IACs, therefore the presence of a pGGN should not be used as an indication for limited resection.

The current study had some limitations. One is that it was retrospective, and another is that all the data were derived from a single institution. All the data in the study were derived from 2016 however, and all patients were managed in accordance with the same protocol; thus, there was conceivably relatively minimal bias. Another potential limitation is that only patients in whom a diagnosis had been established via resection were included, but some of the unresected pGGNs may also have been adenocarcinomas. pGGNs can have non-cancerous origins, most notably infection, among others. These factors may have contributed to a selection bias in the present study. A prospective study would be required to minimize these potential sources of bias. An additional study limitation is that distinguishing between pGGNs and other nodules is subjective. Two reviewers (a radiologist and a surgeon) evaluated all CT scans independently to minimize this source of bias. Lastly, it is not always possible to completely exclude all blood vessels and bronchioles when delineating the boundaries of lesions, and this may have contributed to variations between observers in nodule measurements and the characterization of lesions.

In conclusion, patients with pGGNs < 3 cm in diameter on CT are more likely to have IACs if they are aged > 55 years, exhibit a nodule diameter > 1 cm, and the CT-determined density of the nodule is > − 600 HU. We suggest that surgical treatment and lobectomy is preferable to limited resection in these patients. Postoperatively, IACs initially identified as pGGNs have a good prognosis, and there were no recurrences during a median follow-up period of 41 months in the current study. The results of this study may assist decisions pertaining to the selection of surgical procedures in patients with pGGNs identified as being at high risk of malignant disease.

List Of Abbreviations

pGGNs, pure ground-glass nodules; CT, computed tomography; IACs, invasive adenocarcinoma; HU, Hounsfield units; AIS, adenocarcinoma in situ; MIA, minimally invasive adenocarcinoma; CEA, serum carcinoembryonic antigen; ROC, Receiver operating characteristic; AUCs, area under curves; ORs, odds ratios; CIs, confidence intervals;

Declarations

Ethics approval and consent to participate

The study was conducted in accordance with the Declaration of Helsinki. The Institutional Review Board and the Ethics Committee of Shanghai Chest Hospital approved the study, and waived the requirement for patient consent due to its retrospective design.

Consent for publication

Not applicable.

Availability of data and materials

The datasets used and/or analysed during the current study are available from the corresponding author on reasonable request.

Competing interests

The authors declare that they have no competing interests.

Funding

This work was supported by the Program in Western Medicine approved by Shanghai Science and Technology Commission (16411966000), the Interdisciplinary Program of Shanghai Jiaotong University (YG2014QN22) and Natural Science Foundation of China (81402571).

Author Contributions

(I) Conception and design: Huan-Huan Yang, Yi-Lv Lv, Bo Ye, Ding-Zhong Hu

(II) Administrative support: Ding-Zhong Hu, Bo Ye

(III) Provision of study materials or patients: Huan-Huan Yang, Yi-Lv Lv, Xing-Hai Fan, Zhi-Yong Ai, Xiu-Chun Xu

(IV) Collection and assembly of data: Huan-Huan Yang, Yi-Lv Lv, Xing-Hai Fan

(V) Data analysis and interpretation: Huan-Huan Yang, Yi-Lv Lv, Xing-Hai Fan, Zhi-Yong Ai, Xiu-Chun Xu

(VI) Manuscript writing: All authors

(VII) Final approval of manuscript: All authors

Acknowledgment

We thank Dr Owen Proudfoot from Liwen Bianji, Edanz Editing China (www.liwenbianji.cn/ac) for editing the English text of a draft of this manuscript.

References

1. Matsuguma H, Mori K, Nakahara R, et al. Characteristics of subsolid pulmonary nodules showing growth during follow-up with CT scanning. Chest. 2012;143(2):436–43.
2. Naidich DP, et al. Recommendations for the management of subsolid pulmonary nodules detected at CT: a statement from the Fleischner Society. Radiology. 2013;266(1):304–17.
3. Park CM, et al. CT findings of atypical adenomatous hyperplasia in the lung. Korean J Radiol. 2006;7(2):80–6.
4. Kim HY, et al. Persistent pulmonary nodular ground-glass opacity at thin-section CT: histopathologic comparisons. Radiology. 2007;245(1):267–75.
5. Noguchi M, et al. Small adenocarcinoma of the lung. Histologic characteristics and prognosis. Cancer. 1995;75(12):2844–52.
6. Yim J, Zhu LC, Chiriboga L, Watson HN, Goldberg JD, Moreira AL. Histologic features are important prognostic indicators in early stages lung adenocarcinomas. Mod Pathol. 2007;20:233–41.
7. Borczuk AC, et al. Invasive size is an independent predictor of survival in pulmonary adenocarcinoma. Am J Surg Pathol. 2009;33(3):462–9.
8. Maeshima AM, et al. Histological scoring for small lung adenocarcinomas 2 cm or less in diameter: a reliable prognostic indicator. J Thorac Oncol. 2010;5(3):333–9.
9. Zhang J, et al. Why do pathological stage IA lung adenocarcinomas vary from prognosis?: a clinicopathologic study of 176 patients with pathological stage IA lung adenocarcinoma based on the IASLC/ATS/ERS classification. J Thorac Oncol. 2013;8(9):1196–202.
10. Nakata M, et al. Focal ground-glass opacity detected by low-dose helical CT. Chest. 2002;121(5):1464–7.
11. Lim HJ, et al. Persistent pure ground-glass opacity lung nodules >/= 10 mm in diameter at CT scan: histopathologic comparisons and prognostic implications. Chest. 2013;144(4):1291–9.
12. MacMahon H, et al. Guidelines for Management of Incidental Pulmonary Nodules Detected on CT Images: From the Fleischner Society 2017. Radiology. 2017;284(1):228–43.
13. Travis WD, et al. Introduction to The 2015 World Health Organization Classification of Tumors of the Lung, Pleura, Thymus, and Heart. J Thorac Oncol. 2015;10(9):1240–2.
14. Travis WD, et al. International Association for the Study of Lung Cancer/American Thoracic Society/European Respiratory Society: international multidisciplinary classification of lung adenocarcinoma: executive summary. Proc Am Thorac Soc. 2011;8(5):381–5.
15. Kitami A, et al. Correlation between histological invasiveness and the computed tomography value in pure ground-glass nodules. Surg Today. 2016;46(5):593–8.

16. Hwang IP, et al. Persistent Pure Ground-Glass Nodules Larger Than 5 mm: Differentiation of Invasive Pulmonary Adenocarcinomas From Preinvasive Lesions or Minimally Invasive Adenocarcinomas Using Texture Analysis. Invest Radiol. 2015;50(11):798–804.
17. Heidinger BH, et al. Lung Adenocarcinoma Manifesting as Pure Ground-Glass Nodules: Correlating CT Size, Volume, Density, and Roundness with Histopathologic Invasion and Size. J Thorac Oncol. 2017;12(8):1288–98.
18. Dai C, et al. Clinical and radiological features of synchronous pure ground-glass nodules observed along with operable non-small cell lung cancer. J Surg Oncol. 2016;113(7):738–44.
19. Jin X, et al. CT characteristics and pathological implications of early stage (T1N0M0) lung adenocarcinoma with pure ground-glass opacity. Eur Radiol. 2015;25(9):2532–40.
20. Xiang W, et al. Morphological factors differentiating between early lung adenocarcinomas appearing as pure ground-glass nodules measuring </=10 mm on thin-section computed tomography. Cancer Imaging. 2014;14:33.
21. Lee SM, Park CM, Goo JM, Lee HJ, Wi JY, Kang CH. Invasive pulmonary adenocarcinomas versus preinvasive lesions appearing as ground-glass nodules: differentiation by using CT features. Radiology. 2013;268:265–73.
22. Liu LH, et al. CT findings of persistent pure ground glass opacity: can we predict the invasiveness? Asian Pac J Cancer Prev. 2015;16(5):1925–8.
23. Ding H, et al. Value of CT Characteristics in Predicting Invasiveness of Adenocarcinoma Presented as Pulmonary Ground-Glass Nodules. Thorac Cardiovasc Surg. 2017;65(2):136–41.
24. Callister ME, et al. British Thoracic Society guidelines for the investigation and management of pulmonary nodules. Thorax. 2015;70(Suppl 2):ii1–54.
25. Gould MK, et al., Evaluation of individuals with pulmonary nodules: when is it lung cancer? Diagnosis and management of lung cancer, 3rd ed: American College of Chest Physicians evidence-based clinical practice guidelines. Chest, 2013. 143(5 Suppl): p. e93S-e120S.
26. Lee HY, Lee KS. Ground-glass opacity nodules: histopathology, imaging evaluation, and clinical implications. J Thorac Imaging. 2011;26:106–18.
27. Cho S, et al. Pathology and prognosis of persistent stable pure ground-glass opacity nodules after surgical resection. Ann Thorac Surg. 2013;96(4):1190–5.
28. Lee HY, et al. Pure ground-glass opacity neoplastic lung nodules: histopathology, imaging, and management. AJR Am J Roentgenol. 2014;202(3):W224-33.
29. Ohtsuka T, et al. A clinicopathological study of resected pulmonary nodules with focal pure ground-glass opacity. Eur J Cardiothorac Surg. 2006;30(1):160–3.
30. Yeh YC, Nitadori J, Kadota K, et al. Using frozen section to identify histological patterns in stage I lung adenocarcinoma of </= 3 cm: accuracy and interobserver agreement [J]. Histopathology. 2015;66(7):922–38. doi:10.1111/his.12468.

Tables

Table . Optimal cutoff values for continuous predictors.

Indicator	AUC	p	Cut off value[a]	Sensitivity	Specificity	PPV	NPV
Age (years)	0.704(0.657,0.751)	< 0.001	53	52%	79%	91%	30%
Serum CEA (μg/L)	0.495(0.440,0.550)	0.862	2.19	90%	15%	80%	28%
Max diameter (mm)	0.845(0.805,0.885)	< 0.001	10.78	81%	79%	94%	52%
CT value (HU)	0.664(0.613,0.715)	< 0.001	-582.28	66%	60%	87%	32%
Mean diameter (mm)	0.852(0.813,0.89)	< 0.001	10.09	86%	75%	93%	58%

[a]Cutoff values were determined via the maximal Youden index (sensitivity + specificity − 1).AUC, area under the receiver operating characteristic curve; CEA, carcinoembryonic antigen; CT, computed tomography; HU, Hounsfield units; Max, maximal; NPV, negative predictive value; PPV, positive predictive value

Table . Baseline patient characteristics by diagnostic category.

Variable	Total (n = 659)	Pre-IAC (n = 523)	IAC (n = 136)	χ^2	p
Sex				5.042	0.025
Male	200 (30.3%)	148 (28.3%)	52 (38.2%)		
Female	459 (69.7%)	375 (71.7%)	84 (61.8%)		
Age, years				40.540	< 0.001
≤ 55	325 (49.3%)	291 (55.6%)	34 (25.0%)		
> 55	334 (50.7%)	232 (44.4%)	102 (75.0%)		
Smoking history				4.985	0.723
Never	350 (53.1%)	283 (54.1%)	67 (49.3%)		
Current or former	309 (46.9%)	240 (45.9%)	69 (50.7%)		
Symptoms				5.742	0.831
Absent	480 (72.8%)	410 (78.4%)	70 (51.5%)		
Present	179 (27.2%)	113 (21.6%)	66 (48.5%)		
Serum CEA, μg/L				.069	0.792
< 5	652 (99.1%)	518 (99.2%)	134 (98.5%)		
≥ 5	6 (0.9%)	4 (0.8%)	2 (1.5%)		
Maximal diameter, cm				145.831	< 0.001
≤ 1	430 (65.2%)	401 (76.7%)	29 (21.3%)		
> 1	229 (34.8%)	122 (23.3%)	107 (78.7%)		
Mean diameter, cm				188.727	< 0.001
≤ 1	475 (72.0%)	441 (84.3%)	34 (25.0%)		
> 1	184 (28.0%)	82 (15.7%)	102 (75.0%)		
CT density, HU				21.374	< 0.001
≤−600	344 (52.2%)	297 (56.8%)	47 (34.6%)		
>−600	315 (47.8%)	226 (43.2%)	89 (65.4%)		
Pleural retraction				0.033	0.857

CEA, carcinoembryonic antigen; CT, computed tomography; HU, Hounsfield units; IAC, invasive adenocarcinoma

Variable	Total (n = 659)	Pre-IAC (n = 523)	IAC (n = 136)	χ^2	p
Absent	633 (96.1%)	502 (96.0%)	131 (96.3%)		
Present	26 (3.9%)	21 (4.0%)	5 (3.7%)		
Air bronchogram sign				.000	1.00
Absent	647 (98.2%)	513 (98.1%)	134 (98.5%)		
Present	12 (1.8%)	10 (1.9%)	2 (1.5%)		
Bubble lucency sign				0.278	0.598
Absent	598 (90.7%)	473 (90.4%)	125 (91.9%)		
Present	61 (9.3%)	50 (9.6%)	11 (8.1%)		
Spiculated sign				5.329	0.021
Absent	560 (85.0%)	453 (86.6%)	107 (78.7%)		
Present	99 (15.0%)	70 (13.4%)	29 (21.3%)		
CEA, carcinoembryonic antigen; CT, computed tomography; HU, Hounsfield units; IAC, invasive adenocarcinoma					

Table . Univariable and multivariable analysis of associations between invasive adenocarcinoma and potential predictors thereof. Working correlation structure in the generalized estimation model was determined via quasi-likelihood under the independence model criterion, and unstructured working correlation structure was selected. Multivariable model 1 only included variables whose p values were < 0.1 in the univariable model. Multivariable model 2 included all potential variables, and was performed as a sensitivity analysis.

Characteristics		Univariable model		Multivariable Model 1		Multivariable Model 2	
		OR (95% CI)	p	OR (95% CI)	p	OR (95% CI)	p
Sex	Female	0.634 (0.427, 0.942)	0.024	0.784 (0.468, 1.313)	0.356	0.708(0.415, 1.208)	0.205
	Male	Reference		Reference		Reference	
Age, years	> 55	3.764 (2.464, 5.748)	< 0.001	2.240 (1.370, 3.665)	0.001	2.732 (1.605, 4.651)	< 0.001
	≤ 55	Reference		Reference		Reference	
Smoking history	Current or former	0.801 (0.590, 1.284)	0.722	-	-	0.721 (0.401, 1.023)	0.942
	Never	Reference		Reference		Reference	
Symptoms	Present	1.080 (0.780, 2.196)	0.830	-	-	0.988 (0.697, 2.010)	0.984
	Absent	Reference		Reference		Reference	
Serum CEA, μg/L	> 1	1.932 (0.350, 10.661)	0.45	-	-	0.967 (0.235, 3.978)	0.963
	≤ 1	Reference		Reference		Reference	
Maximal diameter, cm	> 1	13.058 (8.192, 20.814)	< 0.001	2.690 (0.994, 7.276)	0.051	2.992 (1.098, 8.153)	0.032
	≤ 1	Reference		Reference		Reference	
Mean diameter, cm	> 1	16.190 (10.285, 25.486)	< 0.001	6.207 (2.352, 16.383)	< 0.001	4.707 (1.761, 12.583)	0.002
	≤ 1	Reference		Reference		Reference	
CT density, HU	>−600	2.612 (1.756, 3.885)	< 0.001	3.542 (2.155, 5.822)	< 0.001	3.886 (2.307, 6.548)	< 0.001
	≤−600	Reference		Reference		Reference	

CEA, carcinoembryonic antigen; CI, confidence interval; CT, computed tomography; HU, Hounsfield units; IAC, invasive adenocarcinoma; OR, odds ratio (estimated from generalized estimation model)

Characteristics		Univariable model		Multivariable Model 1		Multivariable Model 2	
		OR (95% CI)	p	OR (95% CI)	p	OR (95% CI)	p
Pleural retraction	Present	0.991 (0.329, 2.986)	0.988	-	-	2.042 (0.444, 9.390)	0.359
	Absent	Reference		Reference		Reference	
Air bronchogram sign	Present	0.765 (0.166, 3.535)	0.732	-	-	0.193 (0.042, 0.882)	0.034
	Absent	Reference		Reference		Reference	
Bubble lucency sign	Present	0.824 (0.415, 1.639)	0.582	-	-	0.583 (0.249, 1.365)	0.214
	Absent	Reference		Reference		Reference	
Spiculated sign	Present	1.761 (1.093, 2.838)	0.02	1.445 (0.781, 2.671)	0.241	1.758 (0.880, 3.511)	0.11
	Absent	Reference		Reference		Reference	

CEA, carcinoembryonic antigen; CI, confidence interval; CT, computed tomography; HU, Hounsfield units; IAC, invasive adenocarcinoma; OR, odds ratio (estimated from generalized estimation model)

Table . Multicollinearity test from multivariable models 1 and 2.

Index	Criterion	Multivariable Model 1	Multivariable Model 2
Conditional index	< 10	6.52	6.48
Minimal tolerance	> 0.1	0.26	0.27
Maximal variance inflation factor	< 10	3.83	3.69

Figures

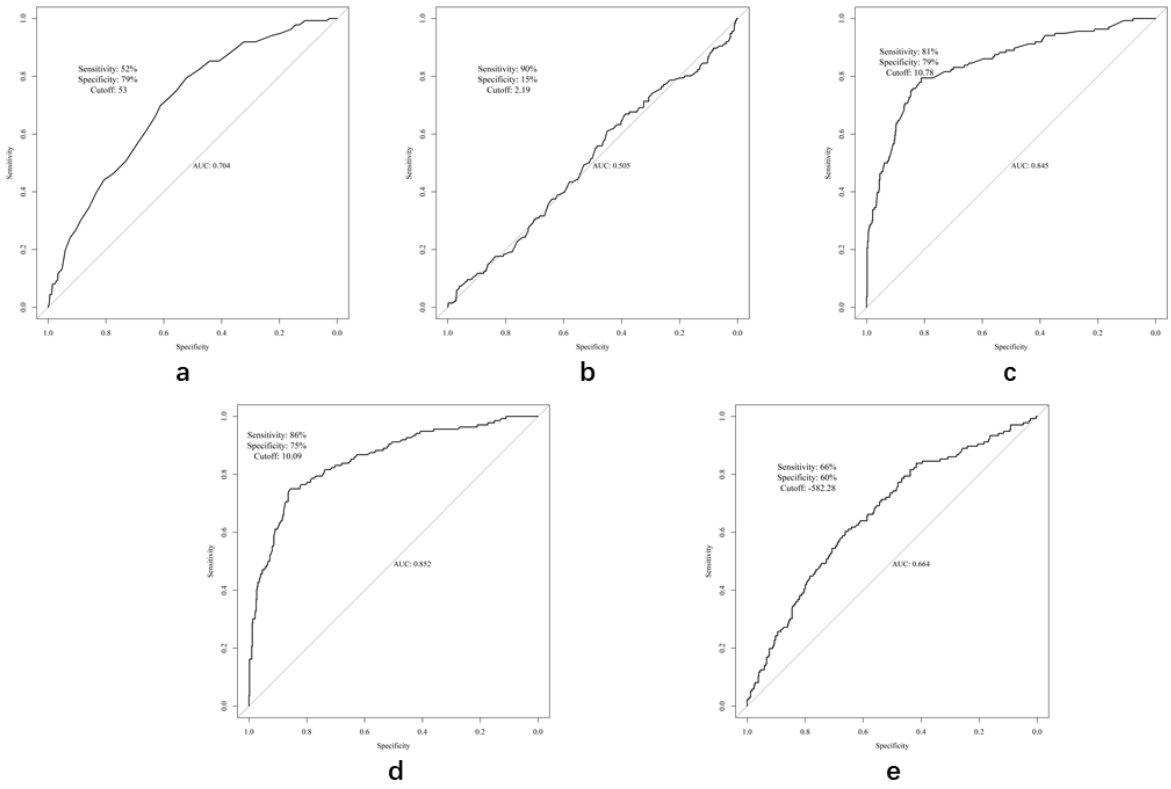

Figure 1

Receiver operating characteristic curves for age (a), serum carcinoembryonic antigen concentration (b), maximal diameter (c), mean diameter (d), and computed tomography-determined density (e)AUC, area under the receiver operating characteristic curve

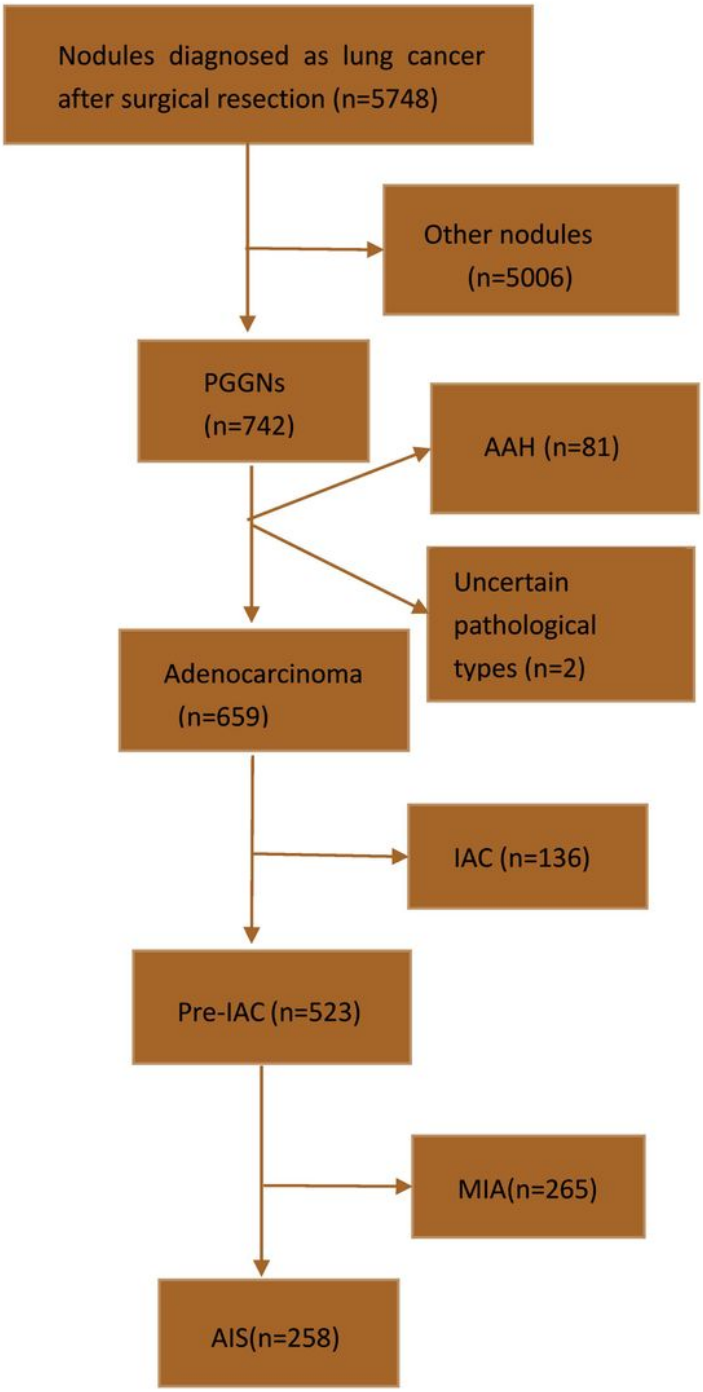

Figure 2

Flow chart and schema depicting the process of classifying nodules as pure ground glass nodules (pGGNs), atypical adenomatous hyperplasia (AAH), invasive adenocarcinoma (IAC), minimally invasive adenocarcinoma (MIA), and adenocarcinoma in situ (AIS)

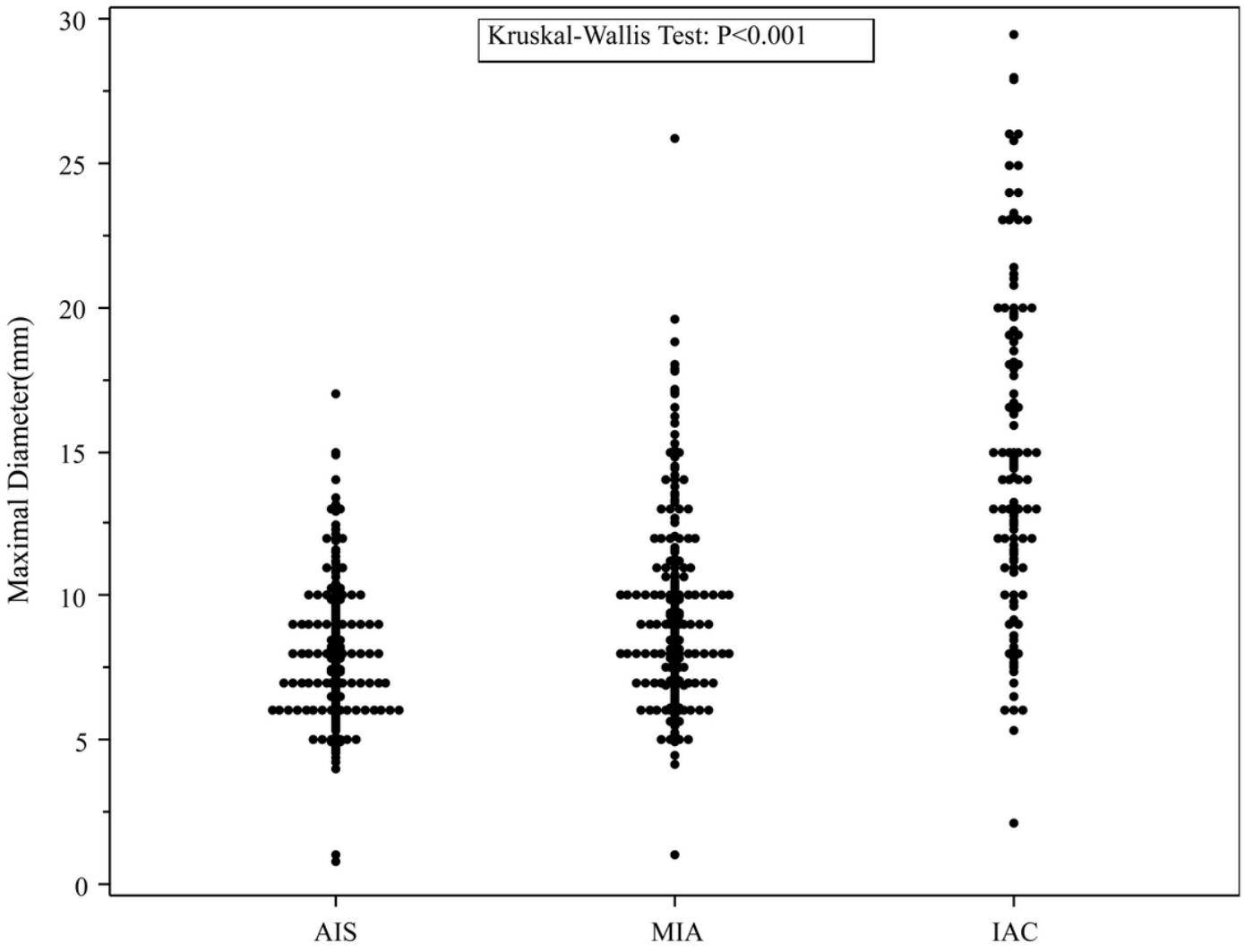

Figure 3

Scatter plot of pure ground-glass nodule maximal diameters determined via computed tomography plotted by pathological type(AIS, adenocarcinoma in situ; IAC, invasive adenocarcinoma; MIA, minimally invasive adenocarcinoma)

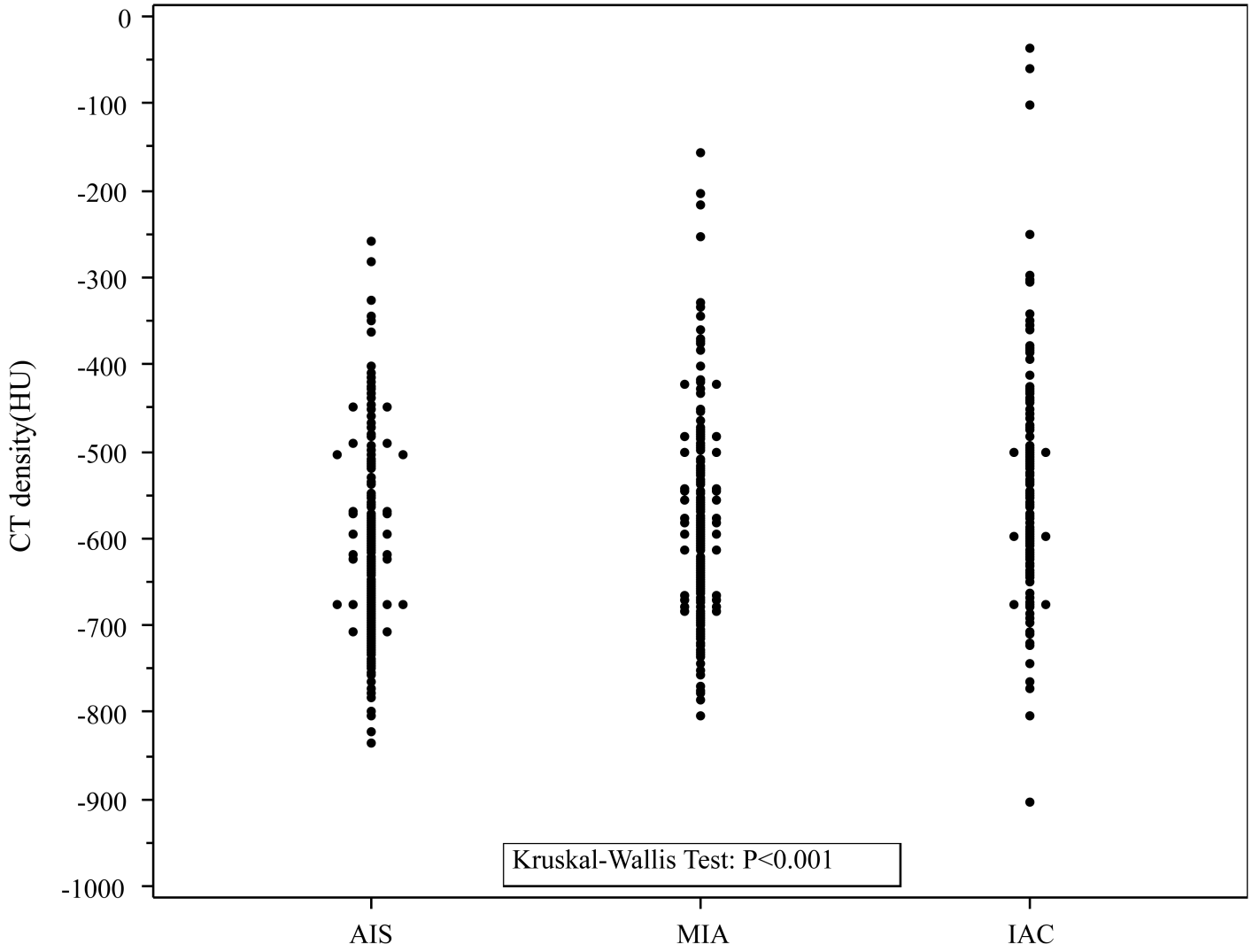

Figure 4

Scatter plot of computed tomography-determined density of pure ground-glass nodules plotted by pathological type(AIS, adenocarcinoma in situ; CT, computed tomography; HU, Hounsfield units; IAC, invasive adenocarcinoma; MIA, minimally invasive adenocarcinoma)

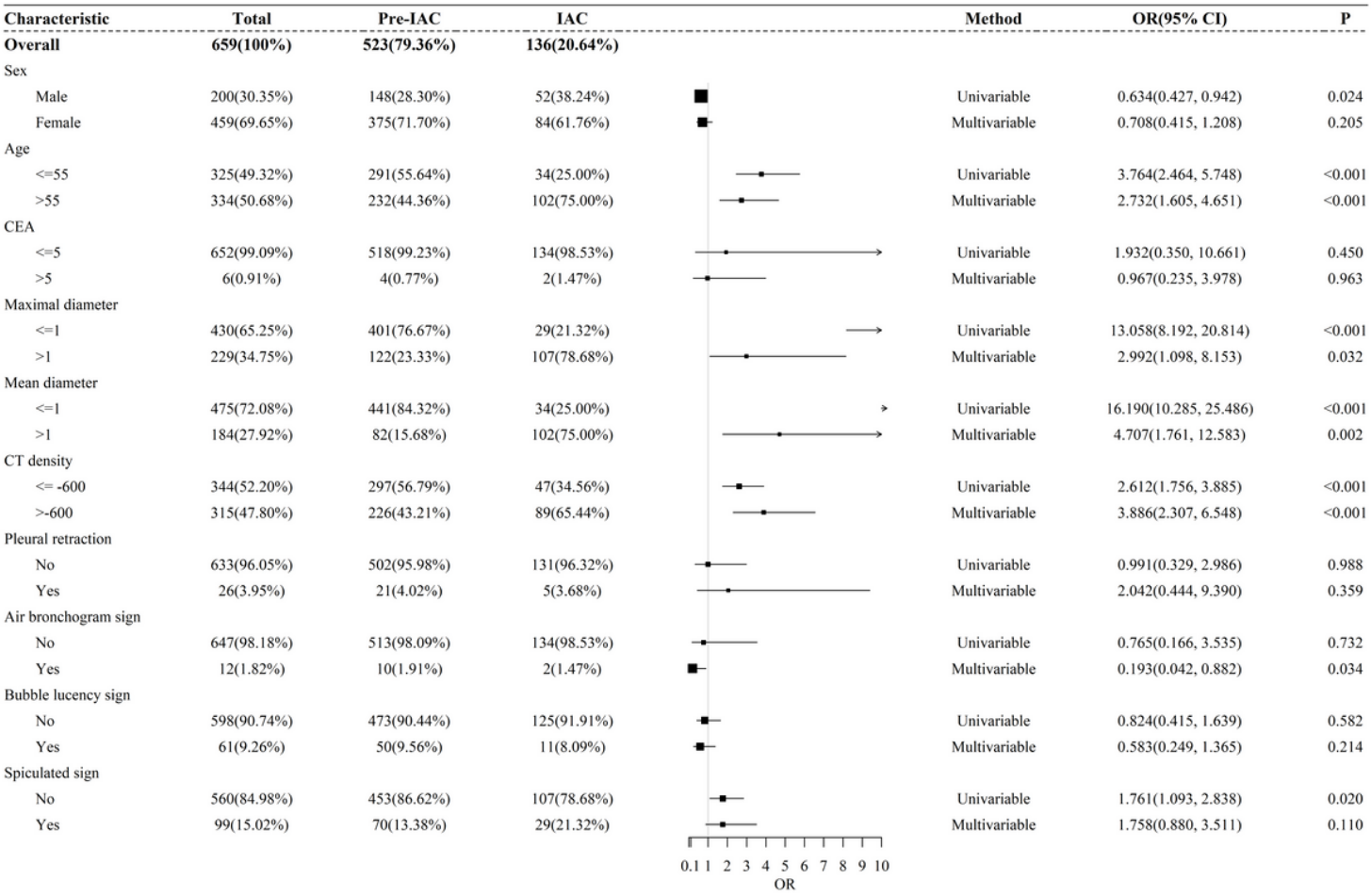

Figure 5

Forest plot of all results of univariable and multivariable analyses

Supplementary Files

This is a list of supplementary files associated with this preprint. Click to download.

- ESMTable1.docx